Report Cover Page & Vehicle Description Form
e-Human Powered Vehicle Challenge

Competition Location: PES University
Bengaluru, Karnataka, India
Competition Date: April 1 – April 2, 2023

This required document for all teams is to be incorporated into your design report.
Please Observe Your Due Dates; see the ASME e-HPVC website and rules for due dates.

Vehicle Description

University name: Delhi Technological University
Vehicle name: ERAWAT
Vehicle number:
Vehicle configuration:
Upright _____ Semi-recumbent Yes
Prone _____ Other (specify) _____
Frame material: Carbon Fibre and Titanium
Fairing material(s): Carbon Fibre and Honeycomb Matrix
Number of wheels: 2
Vehicle Dimensions (m)
Length: 2.894 m
Width: 0.840 m
Height: 1.193 m
Wheelbase: 1.432 m
Weight Distribution (kg)
Front: 45%
Rear: 55%
Total Weight (kg): 28 kg
Wheel Size (m)
Front: 0.410 m
Rear: 0.673 m
Frontal area (m^2): 0.4736 m^2
Steering (Front or Rear): Front
Braking (Front, Rear, or Both): Both
Estimated Coefficient of Drag: 0.06

Vehicle history (e.g., has it competed before? where? when?):
No, the vehicle has not competed in any event at the time of submission of the design report.

Delhi Technological University

2023 ASME Asia Pacific e-HPV Challenge

DELHI TECHNOLOGICAL UNIVERSITY

Introducing

ERAWAT

Team Advisor

Dr. Raghvendra Gautam
Department of Mechanical Engineering
raghvendrag80@yahoo.com

Team Members

Abhinav Kumar Jha	Aryan Gupta	Mehul Agarwal	Utsav Mittal
Aditya Singh	Aryan Nigam	Priyanshu Sinha	Vishal Yadav
Aditya Yadav	Dhruv Goel	Rahul kumar Srivastava	Yash Sharma
Aman Kumar	Harsh Kumar Yadav	Rhythm Aggarwal	Yogender
Arko Sardar	Harshit Chandna	Shubhangam	
Aryan Gupta	Mahatva Anand	Siddharth Garg	

For more information contact,

Siddharth Garg
Captain
officialsiddharthgarg@gmail.com

Mehul Agarwal
Vice-Captain
mehulagarwal11@gmail.com

THREE VIEW DRAWING

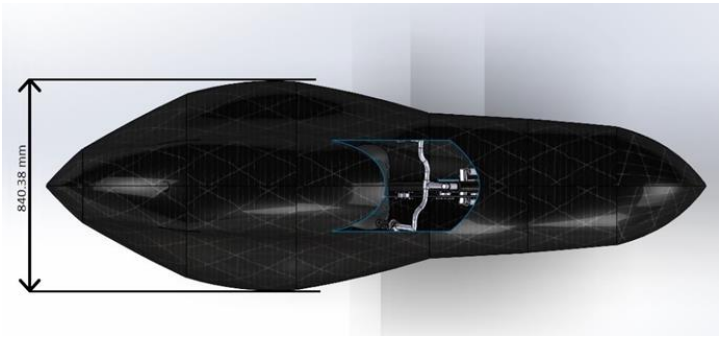

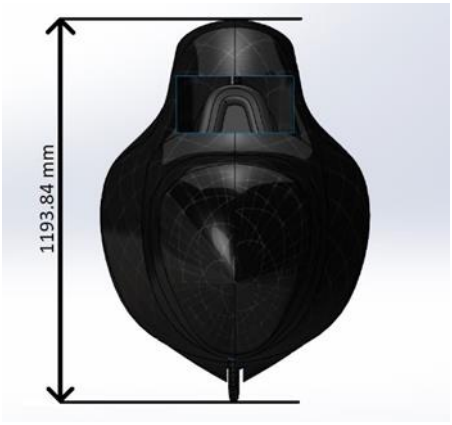

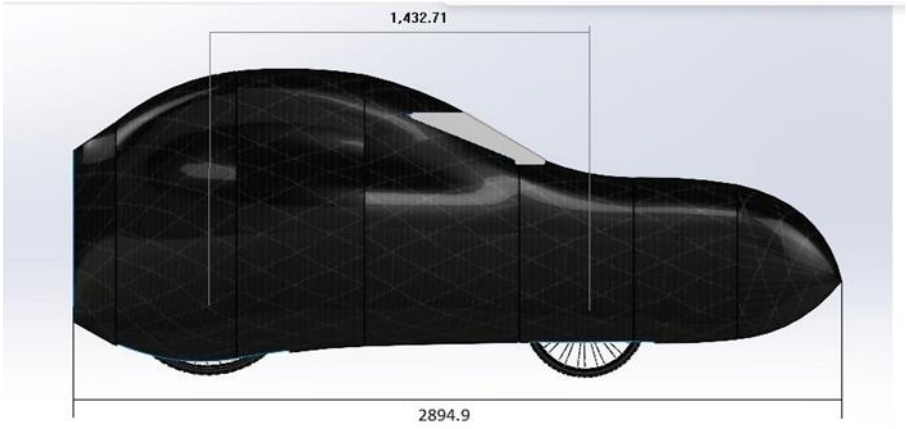

All dimensions are in millimeters.

Dimensioning and tolerancing as per ASME Y14.5 and related standards such as ASME Y14.24 and ASME Y14.3

ABSTRACT

The concept of Human Powered Vehicles (HPVs) has been around for centuries. From the earliest bicycles to modern-day velomobiles, HPVs have evolved into a viable mode of transportation that can offer numerous benefits over traditional automobiles. In recent years, there has been an increased interest in HPVs, driven by concerns over environmental sustainability and the need to find alternative forms of transportation that are both eco-friendly and affordable. This report provides an overview of Team Raftaar's 10^{th} Vehicle ERAWAT, as the team strives to raise the bar in the domain of human-powered vehicles.

Building upon the strong foundation, Team Raftaar, DTU designed, tested and fabricated ERAWAT, a fully-faired lightweight, and efficient e-HPV to compete in ASME EFX India's Human Powered Vehicle Competition (e-HPVC) 2023.

ERAWAT was primarily designed using SOLIDWORKS 2021. ANSYS 22 was used for structural analysis and aerodynamic analysis of the vehicle to ensure that all safety standards set by ASME are met. MSC ADAMS was used for Suspension Analysis and MATLAB Simulink was used for Electrical Analysis of the vehicle. Adequate physical testing was also performed at the necessary stages for the RPS Testing. 3 Point Bend test was done for Frame Selection and Die Penetration Test for Weld Quality check. Wind Tunnel testing of a scaled model was done to verify the simulated results for drag.

The team decided to use Carbon Fibre and Titanium as the frame material. The Back wheel hybrid drivetrain was designed, keeping in mind efficiency and space constraints. The vehicle is engineered with an adjustable seat mechanism that permits the rider with different heights to optimize his position accordingly. The fairing for Falcon was fabricated with Carbon Fibre and Honeycomb matrix, acknowledging the adequate number of layers of both through 12-piece moulds. Seat belt, carbon fibre reinforced polymer roll-bar, rider alert system, emergency power off switch and all other safety equipment, as specified by ASME, are also incorporated.

With a host of innovative and robust features to make rider's experience safer and more enjoyable, ERAWAT aims to better the preceding heights achieved by Team Raftaar and continues to pursue the idea of incorporating HPVs in everyday life with the motto, "Ride with purpose, ride with power".

Table of Contents

Three View Drawing

Abstract

1. Design

1.1. Objective
1.2. Background Research
1.3. Prior Work
1.4. Organizational TimeLine
1.5. Design Specifications
1.5.1. House of Quality
1.5.2. PDS
1.6. Concept Development and Selection Methods
1.6.1. Vehicle Configurations
1.6.2. Frame Material
1.6.3. Drivetrain Alternatives
1.7. Vehicle Description
1.7.1. Frame
1.7.2. Fairing
1.7.3. Drivetrain
1.7.4. Practicality
1.7.5. Environmental Conditions
1.8. Innovation
1.8.1 Accident Alert System SOS
1.8.2 Auto-cutoff System

2. Analysis

2.1. RPS Analysis
2.1.1. Top Load Modelling
2.1.2. Top Load Results
2.1.3. Side Load Modelling
2.1.4. Side Load Results
2.2. Structural Analysis
2.2.1. Bottom Bracket Analysis
2.2.2. Head Tube Analysis
2.3. Aerodynamic Analysis
2.3.1. Front Wind Analysis
2.4. Electrical Analysis
2.5. Cost Analysis
2.6. Other Analysis
2.6.1. Brakes Analysis
2.6.2. Suspension Analysis

3. Testing

3.1. Developmental Testing
3.1.1. Frame Developmental Testing
3.1.2. Fairing Dimensions Testing
3.1.3. RPS Testing
3.1.4. Wind Tunnel Testing

4. Conclusion
4.1. Comparison – Design Goals
4.2. Evaluation
4.3. Recommendations
4.4. Conclusion

References

5. Appendices

5.1 Appendix A- Performance and testing of braking system in HPVCs.

5.2 Appendix B- Force, Static, thermal analysis of Braking system.

5.3 Appendix C- Rider Logbook

5.4 Appendix D- Placement of Suspension

5.5 Appendix E – Crash Detection Test

5.5 Appendix F - Accident alert System SOS and Auto cutoff system code.

1. Design

ERAWAT was explicitly designed for ASME e-HPVC 2023 session. The vehicle was designed and manufactured in house during the academic year 2022-23.

1.1 Objective

The e-HPV Team of Delhi Technological University, Team Raftaar designed and fabricated ERAWAT during the 2022-23 academic year, guided by the team's mission statements:

"*Goal*: To create a revolutionary electric-Human Powered Vehicle that defies convention, blending cutting-edge technology with exquisite aesthetics.

Vision: To offer our team a stimulating and intellectually demanding project that pushes them to expand their existing knowledge and capabilities.

Mission: To challenge the status quo and set a new standard in human-powered transportation."

1.2 Background Research

Extensive research was conducted by our team, incorporating various research articles, social media content, and past reports from ASME-HPVC participants, to gain a comprehensive understanding of the different types of bicycles and trikes. These efforts have enabled us to identify areas of improvement and potential mistakes in the design of our recumbent cycle.

To further enhance our knowledge of vehicle design, suspension, and steering systems, the team members also referred to esteemed publications such as "Race Car Vehicle Dynamics" by F. Milliken & L. Milliken. Moreover, we explored a variety of blogs, research papers and articles to optimize the rider's comfort, drivetrain efficiency, and to develop an extensive electrical system that aligns with our vision for ERAWAT.

1.3 Prior Work

During the previous years, Team Raftaar had conceptualized and constructed several human-powered recumbent cycles such as Aptera, Falcon, Eurus, Kaze, Mach-4, Pegasus, and many others, to participate in HPVC. For the academic year 2022-23, our team's latest creation, ERAWAT, draws inspiration from the best features and mechanisms of our past vehicles.

Some of them are:

a) The ground clearance has been increased, and the seat design has been enhanced to optimize the rider's comfort.

b) To ensure that the vehicle is lightweight and easy to drive, carbon fiber has been utilized for the fairing, and carbon fiber rods have been incorporated into the frame.

c) To maintain consistency and improve efficiency, the team employed the same software for simulation and design, including SolidWorks and Ansys.

d) The design of the fairing was inspired by Falcon 2020 and Aptera 2021, resulting in a sleek and aerodynamic aesthetic that maximizes the vehicle's performance.

1.4 Organizational Timeline

The necessary tasks were stated and planned to maintain a smooth workflow. The Gantt Chart was updated on a regular level to reflect the current and future status and also helped us in improving productivity and making necessary changes to the speed of production.

(P1: Prototype 1) (P2: Prototype 2)

Figure 1: Timeline of the production of ERAWAT

1.5 Design Specifications

The ASME e-HPVC 2023 requirements and any measure to increase rider, team members, and bystander's safety without compromising the performance, stability, and ride quality of the vehicle guided ERAWAT's Design.

	ASME CONSTARINS	**TEAM GOALS**
PERFORMACE	1) Demonstrate stability at 5 km/hr for 30m (fast paced walking speed). 2) Brake from 25 to 0 km/hr in 6 m 3) Turn within an 8 m radius (26.2 ft) 4) Clear a speed bump with maximum height up to 5 cm	1) Total Weight less than 30kg 2) Top Speed of 100 kmph (0-60kmph in less than 16 sec) 3) Easy rider Ingress/Egress 4) Minimize the overall drag experienced by the fairing 5) Create a more efficient drivetrain for achieving higher top speed. 6) Install adjustable seat mechanism to optimize the rider performance. 7) Have a range of more than 35km.

SAFETY	1)Have a Roll-over Protection System (RPS) that will • Produce less than 5.1 cm of total deformation of application of 2670 N of top load (At an angle 12 degree away from the front) • Produce less than 3.8 cm of total deformation of application of 1330 N side load. • No body contact and adequate abrasion resistance in the event of a fall and slide respectively. 2) Include safety harness that holds rider to vehicle during a crash 3) Include Head/Tail light, bell or horn, front/rear/side reflectors. 4) Field of View of at least 180 Degree. 5) Free from sharp edges, open tubes, protruding screws or any other potential hazards. 6) Have a fire protective covering around battery and BMS.	1) The RPS at all points has a reasonable FOS > 3 at all points and the von – misses stress is below the maximum tensile strength. 2) The safety attachment points stay intact in the event of emergency stop, and emergency cut off is easily accessible 3) The steering system remains intact in the event of a crash (Doesn't detach and hurt the rider) 4) The horn, brake lever and screen are easily accessible. 5) No exposed wires and all batteries are located away from the rider. 6) Use commercially available seat harness
RIDER	1)Log a minimum of 30 minutes of vehicle riding experience before the event. 2) The rider must wear appropriate clothing and properly fitting helmets with fastened straps that CPSC Safety Standard for Bicycle Helmet (16 CFR Part 1203)	1) Daily cycling sessions of 30 min each either on trainer or actual cycle to build stamina and endurance. 2) Buying all protective equipment's from authorized stores and products with security marks.

1.5.1 House of Quality

Conclusion from House of Quality: The team considered factors such as Motor, Vehicle weight and Rider satisfaction as the primary focus, followed by Suspension, ergonomics and roll bar strength. This was decided based on the importance rating given to the metrics analogous to the team requirements.

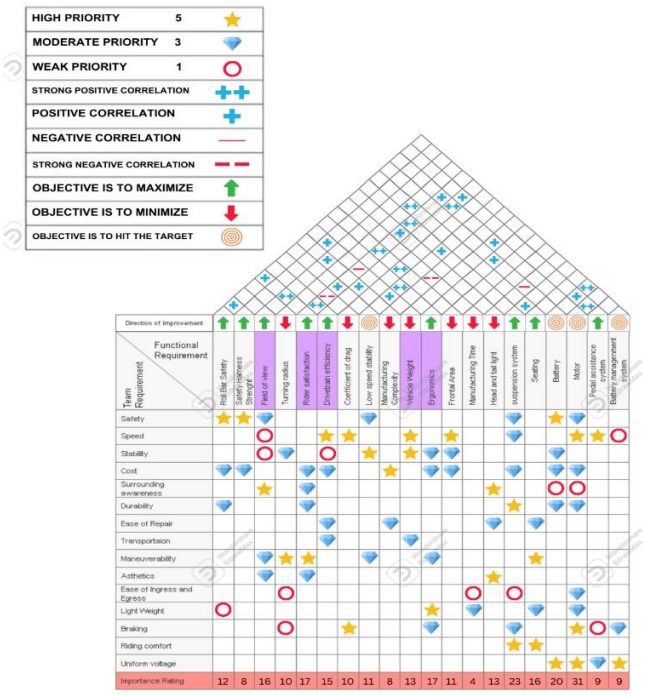

Figure 2: House of Quality

1.5.2 Product Design Specifications

PDS for designing ERAWAT are obtained from the House of Quality and ASME Design constraints as shown:

METRIC	CONSTRAIN
Coefficient of Drag	<0.1
Field of View	180 Degree
Turning Radius	<6m
Cost	<Rs. 5,00,000
Rider Satisfaction	8/10
Weight	<30Kg
Rider Hight Range	15 cm
Braking Distance from 25 Km/Hr	<6m
Low Speed Stability	Stable at 5 Km/Hr for 50m
Range of Vehicle at 500W Driving Power	>35Km
0-60 Km/Hr	<16 sec

Table1: PDS for ERAWAT

1.6 Concept Development and Selection Methods

Based on the design criteria and QFD, the Pugh's concept selection technique was adopted. The team made the decision matrix with a weighted average given to each category for critical design considerations. The team provided a score based on QFD and previous year experience to each category according to the following scoring criteria:

Score	Quality
5	Excellent
4	Good

3	Average
2	Poor
1	Very Poor

Table 2: Scoring Criteria

1.6.1 Vehicle Configurations

The first significant decision to be made was the vehicle configuration. For the same, the team considered various possibilities for vehicle geometry. The most likely possibilities were enlisted and rated according to the criteria discussed in Table 2.

Metric	Weightage (%)	Fully faired recumbent	Partially Faired	Trike	Upright Partially Faired	Tadpole (Recumbent)
Frame weight	15	**3**	4	3	5	2
Aerodynamics	17	**5**	4	3	1	3
Rider Comfort	15	**4**	4	4	3	4
Speed	15	**5**	4	3	2	2
Manoeuvrability	11	**3**	4	4	5	4
Prior Knowledge	13	**5**	4	3	5	2
Drivetrain Efficiency	14	**4**	3	3	5	3
Total	100	**4.19**	3.71	3.26	3.57	2.95

Table 3: Vehicle Consideration Analysis

Finally based on all the above metrics a Fully Faired Recumbent configuration was selected.

1.6.2 Frame Material

Various different metrics were chosen and based on their importance a certain weightage was assigned to them as shown in the table below. As strength to weight ratio is a crucial element for frame, it was given the highest weightage of 40%. A total of 5 suitable materials were compared using a decision matrix.

Metric	Weightage (%)	Mild Steel AISI 1018	Aluminium 6061	Titanium Gr 2 ASTM B265	Carbon Fibre	Carbon Fibre + Titanium (for Joints)
Strength to weight ratio	40	1	3	4	5	**5**
Ease of manufacturing	20	5	4	4	2	**4**
Cost of manufacturing	15	4	3	4	3	**4**
Availability of material	10	5	4	4	4	**4**
Weight	15	2	3	3	5	**5**

Total	100	2.8	3.3	3.85	4.4	**4.55**

Table 4: Decision Matrix for Frame Selection

As shown above, based on the results of the decision matrix a combination of titanium and carbon fibre was selected as the frame material, using titanium at the joints and carbon fibre for connections. The metric value of carbon fibre and the combination of carbon fibre and titanium are close but due to the cost and ease of manufacturing in the combination, the combination of the materials was chosen.

1.6.3 Drivetrain Alternatives

We considered the choice between a Rear Wheel Drive and a Front Wheel Drive, with various possible combinations to consider. Ultimately, we carefully evaluated and selected the most efficient and effective drivetrain components and system configuration to achieve the desired performance and functionality of our recumbent bike.

S.No.	Pedal Powered Directed to	Motor Power directed to	Selected (and Why?)
1.	Back Wheel	Front Wheel	No, if the motor was switched at a different speed than the rear wheel, at a turning point on track, the wheel would slip and immediately lose traction. This could prove dangerous for the rider's safety.
2.	Front Wheel	Front Wheel	No, weight distribution of the components will be unequal. Most of the weight will be focused on the front wheel which will make it difficult to the steer the vehicle
3.	Front Wheel	Back Wheel	Yes, we tried this model on the Prototype 2 of ERAWAT and encountered issues which are mentioned below.
4.	Back Wheel	Back Wheel	Yes, this model was selected as the most appropriate for the safety of rider and efficiency.

Table 5: Various Possible Drivetrain Systems

Figure 3: Prototype 2

Figure: Drivetrain of ERAWAT

Prototype had a FWD system powered by Pedal and a RWD powered by an Electric motor. The front wheel drive system was designed to provide the necessary power to propel the bicycle forward while the rear wheel electric motor was intended to provide additional power

and assist the rider when needed. However, during testing, we encountered two major issues with this system.

1) Front and rear wheels had different speeds, resulting in an unbalanced and jerky ride experience.

2) Chain path in the FWD system limited the turn radius of the front wheel, making it difficult to manoeuvre in tight spaces.

1.7 Vehicle Description

1.7.1. Frame

Based on the results of the decision matrix a combination of Titanium and Carbon fibre was selected as the frame material.

Parameter	Value
Wheelbase	1.474m
Front-wheel diameter	0.41m
Rear wheel diameter	0.673m
Kingpin Angle	18°
Camber	0°
Caster	18°
Steering Axis Angle	72°
Trail	0.05 m

Design of frame:

ERAWAT is a fully faired recumbent bicycle manufactured using Carbon Fibre and ASTM B265 Titanium Grade 2. A short wheelbase of length 1.474m was chosen to ensure good maneuverability and a good turning radius. The ground clearance is kept as 0.19m, optimized to have good stability and avoid breakers.

Manufacturing of frame

The manufacturing of frame involved three steps:

STEP 1: Welding of Titanium Joints.

STEP 2: Joining Carbon Fibre Rods (ID 38mm) by sliding in Titanium Joints (OD 38mm) and using Araldite as adhesive.

STEP 3: Covering the joint with 2 Layers of Carbon Fibre Cloth (2 GSM) with Epoxy as adhesive.

Figure 4: Various steps in the process of Frame Manufacturing



1.7.2 Fairing

The fairing of the Vehicle was made from Carbon Fiber using vacuum bagging and conventional hand layup techniques. High emphasis was placed on the aerodynamic stability of the Vehicle. The final fairing design was achieved after 8 iterations.

The designing process involved using a Java Applet named JAVAFOIL, on which NPL ECH and NACA 6 series were considered for the sections of the vehicle. The ECH 2560 met the needs of the team dimensionally for the top section of the fairing. These sections were further modified to achieve close to the ideal fairing design as per various articles and reports that were studied during background research.

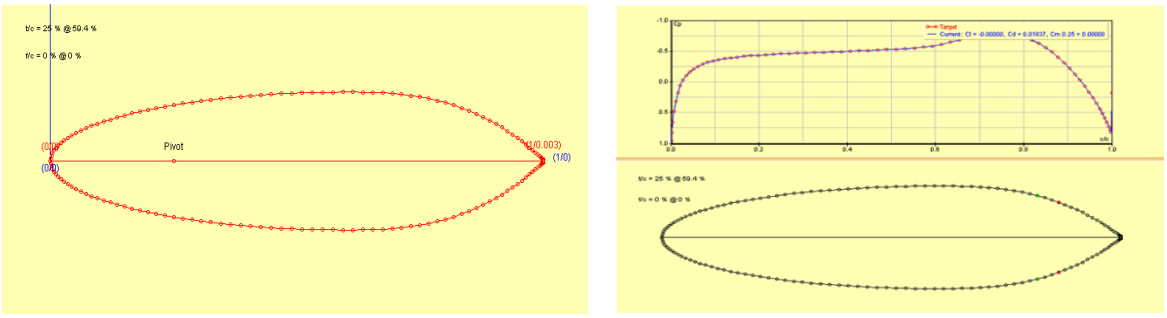

Figure 5: JAVAFOIL modelling ECH2560

Rib placement was given a special emphasis to form a structural member throughout the vehicle. Ribs made of Honeycomb matrix were strategically placed along the regions which must be cut, e.g., the front wheel and windshield cutouts, and along the RPS, where the rider's movement is not obstructed, and where the rider is to be seated.

The fairing's removable top hatch is mainly for the ingress/egress of the rider. Even after the removal of the top hatch, the rider is protected by the fairing RPS in the event of a crash.

12-Piece Mold

The Team decided to change the 10-piece mould we use to a 12-piece mould. Better surface smoothness was one of the major benefits of smaller mould sizes that outweighed its other drawbacks. Moreover, a smaller mould size permits the infusion meshing procedure to produce superior results.

The team fabricated a fully-faired carbon fiber fairing using six female molds on the upper half and six female molds on the lower half fabricated of Glass Fiber (1 layer Chopped sandwiched between 2 layers of Woven) and Gel Coat Epoxy (for smoother surface) inside which carbon fiber was laid up. The team considered the method of infusion meshing rather than the usual hand layup because of its several advantages of it, including better quality, good interior finish, faster cycle time, and lower cost. The justification of the twelve-piece mold is supported by the fact that the larger molds may not get the epoxy binder distributed equivalently using the infusion meshing technique. The above choice was made after the layup testing was done, using infusion meshing on the test piece. CBF (car body filler) was used at places with severe depressions, and the molds were sanded with different grit sizes of sandpaper ranging from 120 to 1500 to get the perfect surface finish to the molds for Carbon Fiber Layup.

Figure 6: Shell Pattern for ERAWAT

1.7.3. Drivetrain

ERAWAT features a RWD system with a Hub Motor, replacing the BLDC motor mounted on the cycle frame in our previous prototype. This change in design allowed for a more efficient and streamlined system, with the motor and wheel working together seamlessly to provide a smooth ride experience. As the rear wheel is the driven wheel, it can be powered by the pedal and electric motor in a more synchronized manner, eliminating the speed difference issue that was present with the front-wheel drive system. This also increased the turning radius of the vehicle in turn increasing its manoeuvrability.

1.8 Innovation

ERAWAT has been equipped with a host of innovative features which the team conceptualized and designed throughout the development phase. The Accident Alert System employed in the vehicle is a low-cost solution to the problem of road accidents. The system is designed to detect accidents and send alerts to emergency services and relatives/friends of the victim(s) through SMS messages. The Auto Cut-off System is also incorporated in case of a crash.

1.8.1 Accident Alert System (SOS)

The aim of this project is to design an Accident Alert System using Arduino MPU6050, GPS and GSM module. The purpose of the system is to detect accidents and send alerts to emergency services and relatives/friends of the victim(s) through SMS messages.

Working: [Refer to Annexure E for the working code of the system]

The system works by continuously monitoring the vehicle's movements using the MPU6050 sensor. When an accident occurs, the MPU6050 detects the sudden change in the vehicle's acceleration and sends an interrupt to the Arduino. The GPS module is then used to get the vehicle's current location and the information is sent to the GSM module using the Arduino. The GSM module then sends an alert SMS message to the emergency services and the victim's relatives/friends. The alert SMS message contains the location of the accident and a request for immediate help.

The system also includes an LED and a buzzer that are used to indicate the status of the system. When the system is turned on, the green LED is turned on and the buzzer sounds a beep. If an accident is detected, the red LED is turned on and the buzzer sounds continuously until the system is turned off.

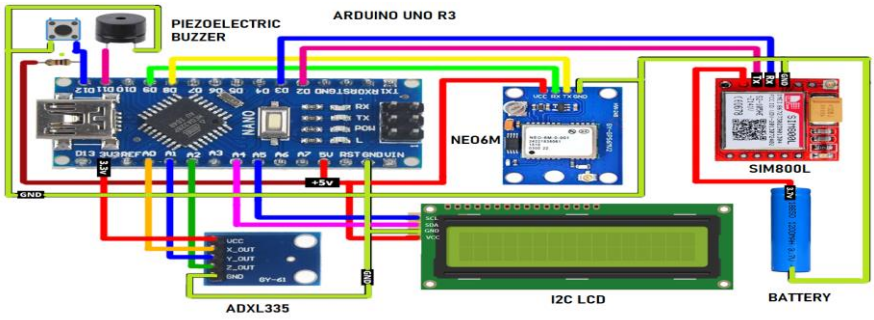

Figure 7: Circuit Diagram of the Accident Alert System

The system is easy to install and can be used in all types of vehicles. The system can save lives and reduce the number of fatalities caused by road accidents.

1.8.2 Auto-Cut-off system

An auto cut-off system is used that detects the tilt of the bike and turns off the battery supply if it tilts more than a specific angle. The system can be easily integrated into the bike's existing electrical system, and it does not require any significant modifications to the bike. The system uses an accelerometer sensor to detect the tilt angle and an Arduino microcontroller to process the data and control the battery supply.

Methodology

The system uses an accelerometer sensor to detect the tilt angle of the bike. The accelerometer sensor is connected to the Arduino microcontroller, which processes the data and controls the battery supply. The Arduino microcontroller is programmed to read the data from the accelerometer sensor continuously and compare it with a present threshold value. If the tilt angle exceeds the threshold value, the microcontroller sends a signal to the battery supply control unit, which turns off the battery supply. The system can be further improved by adding additional sensors and integrating it with the bike's GPS system to provide real-time location-based services.

2. Analysis

2.1 RPS Analysis

Objective	Method	Results
The analysis of the Roll-over Protection System was aimed at the verification of design and ensuring rider safety in accordance with the ASME HPVC guidelines.	This was undertaken in ANSYS 2022 Composite Pre-Post and subsequent FEA was performed with the specific loading conditions as mentioned in the guidelines.	The RPS meets the required specifications with a top and side load deflection of 1.9166 cm and 1.0271 cm respectively.

RPS Description and Attachment

Considering the safety of the rider to be of utmost priority, ERAWAT incorporates a strategically designed roll bar to prevent the rider from direct contact with the road surface and to reduce the impact of any accidental collision.

Finite Element Analysis (FEA) in ANSYS 2022 Composite Pre-Post (ACP) was used for roll bar design in ERAWAT. The finite element model was developed using shell elements in the ACP system. Due to the rollover protection system (RPS) being also supported by the fairing, the analysis of the RPS was performed on ERAWAT's fairing.

2.1.1 Top Load Modelling

A top load of 2670 N was applied to the top of the roll bar, directed downwards and aft at an angle of 12 degrees from the vertical towards the rear of the vehicle with assumption that the seat belt attachment point as a fixture and will be subjected to a reactant force. When the vehicle is subjected to a top load, the load is distributed from the ground to the fairing (Integrated RPS), then to the side rods and the bottom of the frame (both containing the seat belt attachment point). Thereby, protecting body contact from the ground.

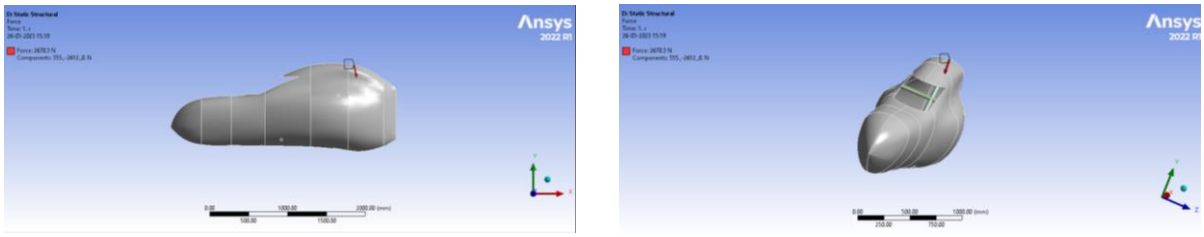

Figure 8: Top Load Modelling

2.1.1 Top Load Results

There is no indication of permanent deformation, fracture or delamination. The maximum elastic deformation as per the analysis carried out is 1.9166 cm which is less than the maximum allowable deformation of 5.1 cm, meeting ASME specification. This gives an FOS value of 2.66.

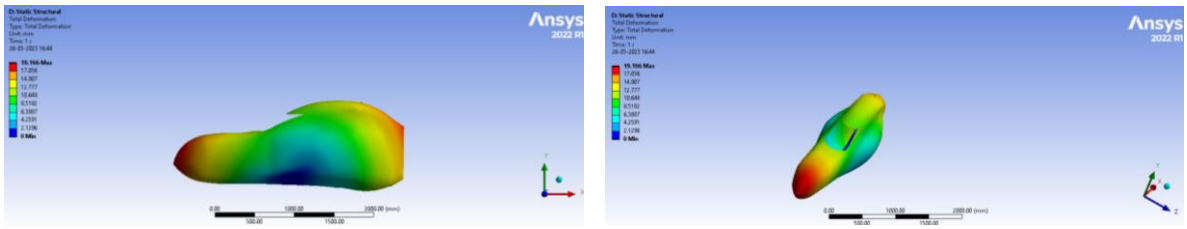

Figure 9: Total Deformation under action of top load

2.1.2 Side Load Modelling

A load of 1330 N was applied horizontally to the side of the roll bar at shoulder height with the assumption that the seat belt attachment point is a fixture and will be subjected to a reactant force. When the vehicle is subjected to a top load, the load is distributed from the ground to the fairing (Integrated RPS), then to the side rods and the bottom of the frame (both containing the safety harness attachment point). Thereby, protecting body contact from the ground.

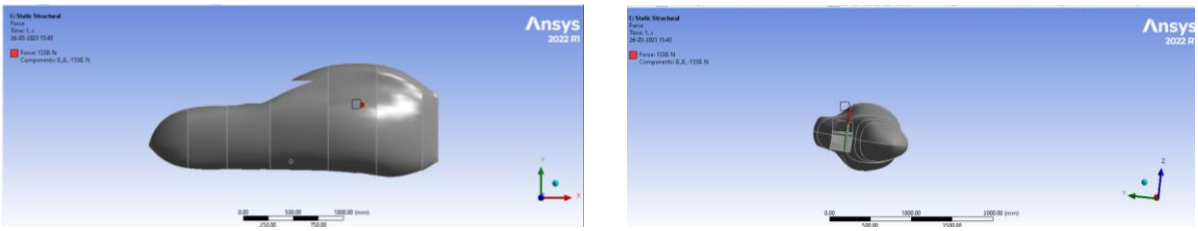

Figure 10: Side Loading of RPS

2.1.3 Side Load Results

There is no indication of permanent deformation, fracture or delamination. The maximum elastic deformation as per the analysis carried out is 1.0271 cm which is less than the maximum allowable deformation of 3.8 cm, meeting ASME specification. This gives an FOS value of 3.70.

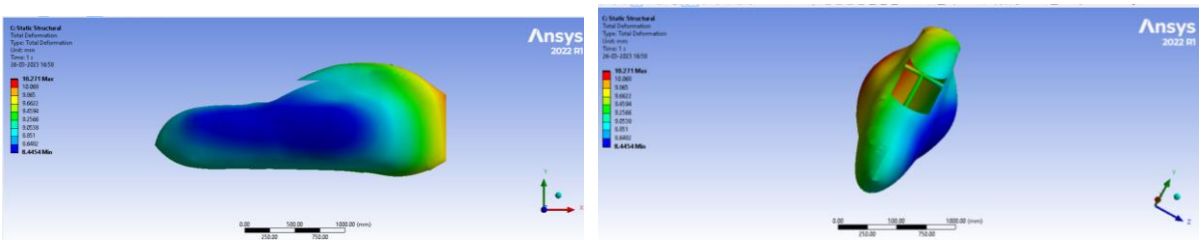

Figure 11: Total Deformation under action of side load

2.2 Structural Analysis

Objective	Method	Results
Modifying the frame after considering various stress scenarios to make a safe and durable vehicle.	Analysis of the Frame was done on ANSYS 2022 to measure the stresses and the strain energy stored within the body under application of the specified loads.	The frame was successfully optimized to withstand all the stress scenarios and to maintain a high Factor of Safety.

Structural Analysis on the frame using ANSYS 2022 were carried out measuring the ability of the frame to withstand various stress scenarios which the vehicle may undergo during its normal operation. All the forces are assumed to be below the elastic limit of the material. (Hooke's Law in 3D). The material of frame considered for the analysis was Titanium Grade E2 ASTM B265.

2.2.1 Bottom Bracket Analysis

Various stresses considered on the bottom bracket include scenarios where the chain experiences large tension force, where there is sudden obstruction leading to considerable friction during the rotation of the pedals, etc. These situations were modeled on Carbon fiber with titanium at joints. An automated mesh has been developed with an average orthogonal quality of 0.856. A Remote force of 650 N was applied along the Z axis at the (0,0,150) mm from the reference coordinate on the center of bottom bracket is shown below. The maximum (Von-Mises) stress is 153.47 MPa was observed in the upper section of the Bottom Bracket Coupler showing that there is a factor of safety (FOS) greater than 2.

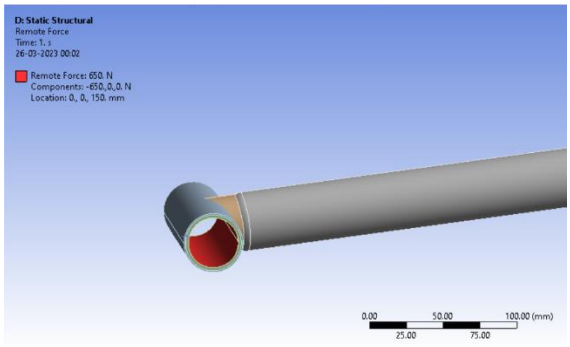

Figure 12: Remote force on the Bottom Bracket Clamp

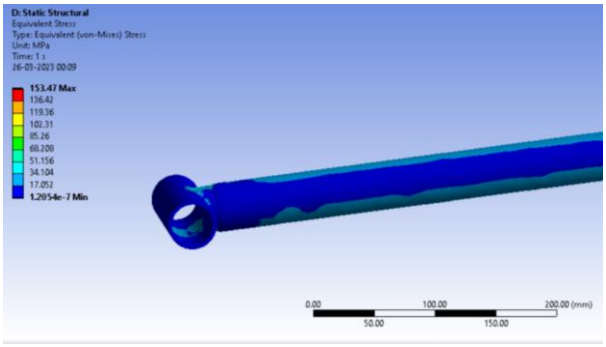

Figure 13: Von – Mises Stress on the Bottom Bracket Clamp

2.2.2 Head Tube Analysis

A significant step to integrate a human-powered vehicle is to ensure that rider comfort is maintained even in rough terrains. The velomobile must be capable of withstanding minor obstacles such as road bumps (with heights up to 9 cm), gravel, sinks and small puddles. An automated mesh has been developed with an average orthogonal quality of 0.864. A compressive force of 2802 N along head tube's axis and a remote force of 1200 N at coordinates (-2033.8, -6259.5, 0) from the global coordinates along x-axis considering center of the head tube as the reference point. These forces were applied on the head tube and the deflection produced was analyzed in the event of a road bump. The frame displays a total deformation of 2.2 mm and has a factor of safety greater than 1. The loading conditions were done according to ASTM F2273-11.

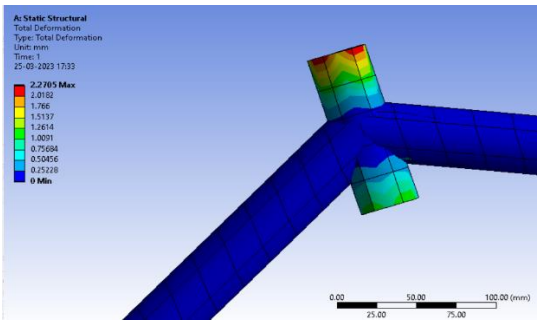

Figure 14: Total Deformation

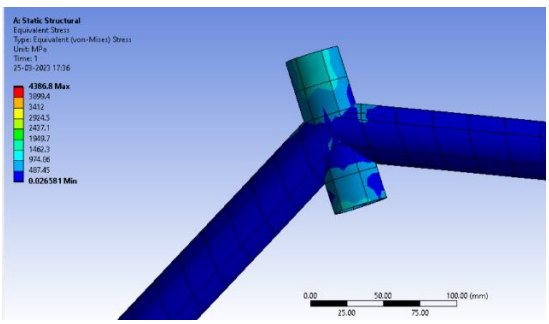

Figure 15: Equivalent (Von-Mises) Stress

2.3 Aerodynamic Analysis

2.3.1 Front Wind Analysis

Objective	Method	Results
To enhance the aerodynamic stability of the fairing to achieve greater overall results.	Analysis was done on Ansys 2022 with multiple iterations incorporating every result into the next iteration.	The C_d of the final iteration came out to be 0.06

Using CFD, the front wind analysis of the draft fairing was done in Ansys Fluent and it yielded a drag coefficient of 0.114 (First Iteration) when the maximum speed was assumed to be 20 m/s (72 kmph). An Ansys recommended guide towards domain sizing was followed.

For CFD, high emphasis was given on the mesh, every mesh metric was checked so that any inaccuracy can be avoided so that the entire process shouldn't be revisited again. RANS based K-Omega Turbulence Model in Steady State, with all y+ wall treatment was chosen as it is not very much memory-intensive and yields good convergence even with complex geometries. The model also proved to be stable under high under relaxation factors which also helped us in observing faster convergence without losses in accuracy.

In the final iteration, the drag coefficient came out to be 0.06 which was much lower than the 1st Iteration.

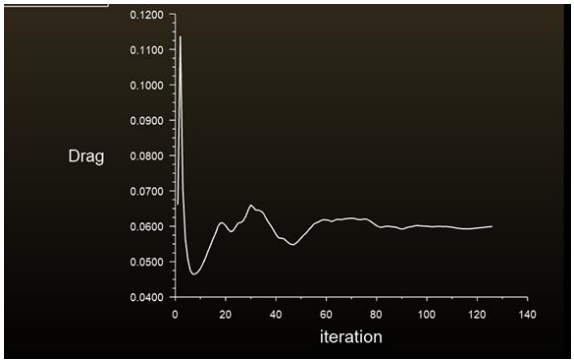

Figure 16: C_d v/s Iteration

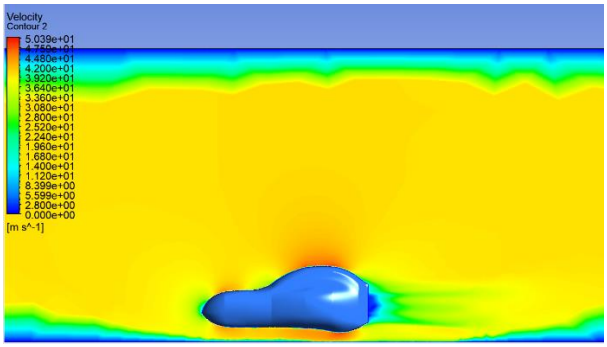

Figure17: Velocity contour in a 3D Analysis

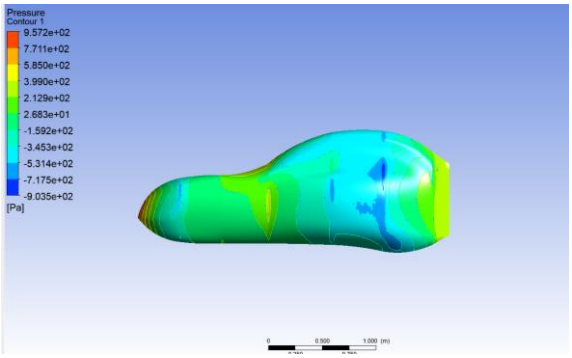

Figure 18: Pressure contour in 3D Analysis

2.4 Electrical Analysis

When it comes to designing successful electric vehicles, one of the biggest challenges is accurately determining their range. Fortunately, with the help of MATLAB Simulink, we have been able to construct a comprehensive simulation environment that considers a variety of easily accessible parameters to provide essential outputs and graphs.

Figure 19: MATLAB Simulink Model

Figure 19: MATLAB Simulink Model

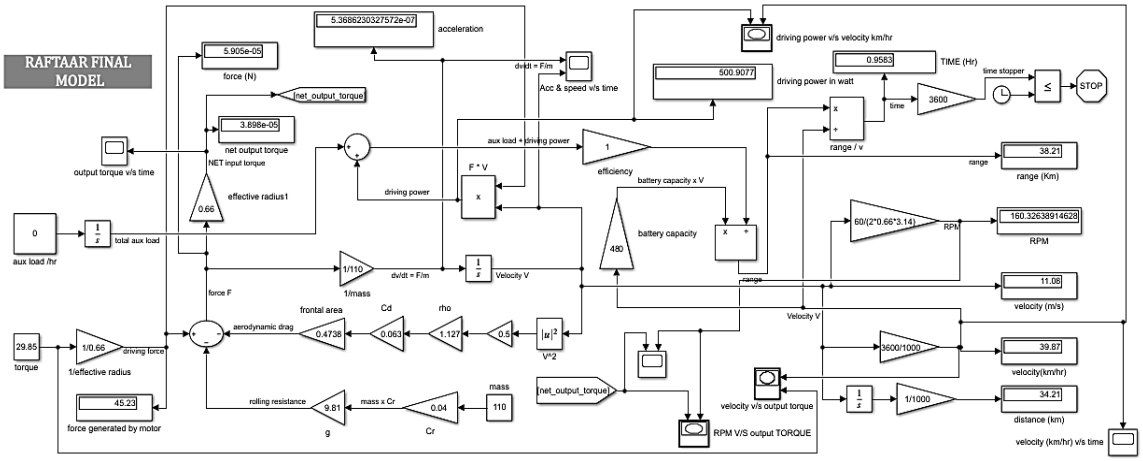

Our Simulink model allows us to determine crucial parameters such as the range of the vehicle, the driving power required to be extracted from the motor, as well as the vehicle's velocity and RPM. These values are obtained through the use of variable input torque, the mass of the vehicle (including the driver), the coefficient of drag, the frontal area of the faring, and the coefficient of rolling resistance.

Functioning of Simulink Model

a) First, we calculate the net force required to propel the vehicle by subtracting the aerodynamic drag and rolling resistance from the input rotating force (Torque * Radius of the wheel).
b) Using the net force, we determine the velocity of the vehicle and connect this velocity as an input to extract the aerodynamic drag, creating a closed loop system.
c) Next, we multiply the input force and velocity to determine the driving power required by the motor. We operate this driving power with an auxiliary load and derive the final power required by multiplying it with the optimum efficiency. In our model, the auxiliary load is zero and efficiency is 1.
d) Finally, we operate the final required power with the product of battery capacity and velocity to determine the range of the vehicle.
e) We also analyze various graphs and parameters to evaluate the performance of the vehicle.

By following these steps, we are able to accurately determine the power and range of the vehicle in a comprehensive manner.

$$Range = \frac{(Battery\ Capacity \times Velocity)}{(Driving\ Power + Aux\ Load) \times \eta}$$ Driving Power=Input Force ×Velocity

$$Net\ Force = Input\ Force - (Aerodynamic\ Drag + Rolling\ Resistance)$$

MATLAB Simulink Model and Graphs

1. **Range calculator whole Simulink model**

In this Simulink model input values are:

- Mass = 110 Kg (including driver's weight)
- Frontal Area = 0.473m^2
- Input torque = variable (in range 28.5 – 32)
- Aux load = 0
- Efficiency,η = 1

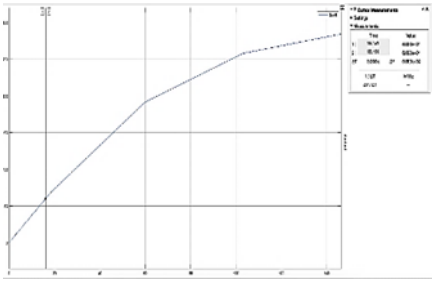

Figure 20: 0-60km/hr in 16.151seconds

2. **0 – 60 Km/Hr in 16.151 seconds:** From this graph we try to obtain that at maximum instant torque our vehicle took 16.151 seconds to attain 0-60 Km/Hr.

3. **Output torque v/s RPM:** It helps us to visualize and understand that, decrease in the output torque due to increase in the aerodynamic drag causes to increase in the RPM of the vehicle.

4. **Net output Torque and RPM v/s Time:** Here, we have presented the variations of torque and RPM with respect to time on a scope. This enables us to determine both values at specific intervals of time.

5. **Acceleration and velocity v/s time:** similarly, here also we depict that acceleration and velocity on the scope which is varying with time. Here we may understand that acceleration is constant, and velocity also becomes constant after achieving its maximum value at a particular torque.

6. **Input Torque v/s RPM v/s Range:** At last, we have calculated the essential parameters like RPM, driving power, Range, and velocity at variable torque and shown in the below table. As well as we made a graph, in which we tried to show the trends of Range and RPM w.r.t torque. In this we also determined that at the rated power of the motor (500W) the range of the vehicle is around 38.21Km.

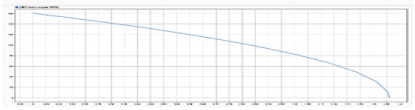

Figure 21: Output Torque v/s RPM

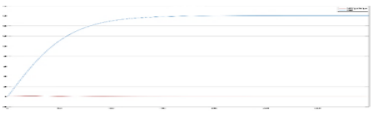

Figure 22: Output Torque and RPM v/s Time

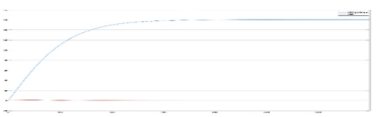

Figure 23: Output Torque and RPM v/s Time

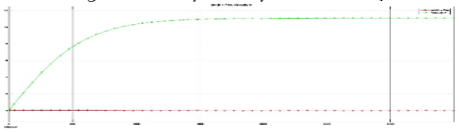

Figure 24: Acceleration and velocity v/s

S.NO.	TORQUE	RPM	VELOCITY (KM/HR)	RANGE	DRIVING POWER
1	28.5	7.64	1.90	40	22.79
2	28.3	76.265	18.97	39.6	229.89
3	29.1	107.4	26.71	39.19	327.12
4	29.4	131.7	32.75	38.79	403.66
5	29.7	151	37.55	38.4	470.13
6	29.85	160.32	39.87	38.21	500.9
7	30.1	174.42	43.38	37.89	549.515
8	30.4	190	47.25	37.52	604.43
9	30.7	204.3	50.81	37.15	656.55
10	31.1	222	55.21	36.67	722.75
11	31.4	234.4	58.29	36.32	770.48
12	31.7	246.3	61.25	35.98	816.94
13	32	257.5	64.04	35.64	862.32

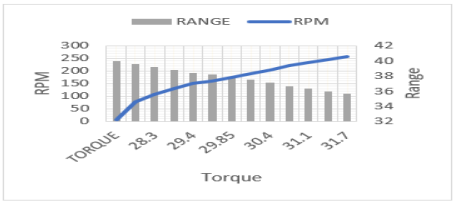

Figure 25: Input Torque v/s RPM v/s Range

2.5 Cost Analysis

Objective	Method	Result
To determine the cost of manufacturing	The Team kept track of all their incurring expenses using a Money Management Software called Buxfer.	The cost of manufacturing of vehicles (excluding student labour) is INR 4,99,300.

All the incurring expenses in the development of the vehicle were segregated and tabulated as shown.

Section	Cost (INR)
Tools & Equipment	18,000
Frame	35,000
Innovation Electronics	9,000
Electrical	33,000
Drivetrain	11,000
Fairing Fabrication	3,20,000
Tyres	6,000
Suspension	2,000
R&D	60,000
Brakes	2,300
Seat	3,000
Total	4,99,300

Figure 26: Cost Analysis of ERAWAT

2.6 Other Analysis

2.6.1 Brakes Analysis

Our objective is to make a type of braking system, which will store the energy which is dispersed or lost while braking, that is Regenerative Braking. Apart from that the team used Disc Brakes on both brakes instead of V-Brakes as used in previous years. [Refer Appendix A]

For Regenerative Braking, Regenerative supporting Motor controllers along with connecting wires are used. During Braking, when brakes are applied microcontrollers disconnect the battery from motor, and make the motor as generator, momentum of the wheels provide energy to the motor thereby storing energy to battery.

Regenerative brakes analysis was done on Simulink MATLAB (Graph 1 shows speed, Graph 2 shows Current, Graph 3 shows Power)

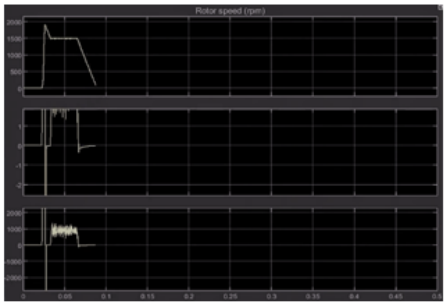

Figure 27: When Mild Brakes are

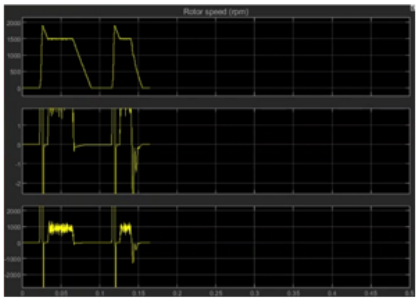

Figure 28: When Heavy Braking is applied

Force, Static and Thermal Analysis

For force analysis on brakes refer Appendix B.

2.6.2 Suspension Analysis

Our primary objective was to ensure rider's safety and enhance the comfort. We aimed to provide a stable structure to the vehicle by deciding a suitable place for back suspension. Moreover, we have used Ansys and MSC Adams software for the analysis part. We have installed two thin carbon fibre plates in between the frame and the supporting rods. The seat stay is now not directly connected to the frame but instead connected to the carbon fibre plates through the suspension. By doing so, we made this a three bars structure at the bottom which provides stability. One of the bars containing suspension is having variable length due to which angle at hinge changes resulting in low stress formation. Suspension was also incorporated into Front folks (Refer Appendix D) for the first time to increase riders' comfort over rough terrain.

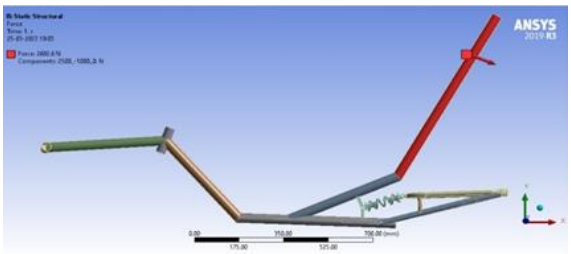

Figure 30: Optimized placement of suspension incorporated

To optimize the placement of suspension for maximum shock absorption research and analysis was conducted on our previous vehicle's frame. Refer Appendix D for this work.

3. Testing

3.1 Frame Developmental Testing

3.1.1 Dye penetration test

This test was performed to check welding surface defects such as cracks and porosity which may be regions of stress concentration and may lead to failure in the long run. (as observed in Prototype 2)

Method:

1. Pre- Cleaning and application of dye
2. Removal of excess dye and application of developer
3. Inspection (Red Spots refer to defects)

The team performed this test on Aluminium (Prototype 2) and Titanium (Final vehicle). Below attached are photos of the test for both materials.

Aluminum 6061

Figure 31: Application of dye

Figure 32: Application of developer

Figure 33: Inspection

Result for Aluminum 6061: The red spots in the above photo are an indication of defects in aluminum.

TITANIUM GR2 ASTM B265

Figure 34: Application of dye

Figure 35: Application of developer

Figure 36: Inspection

Result for Titanium GR2 ASTM B265: The welding/ surface defects in titanium are much less than that (almost negligible)

3.1.2 3-Point Bend Test

This test was performed to find out flexural strength of different materials by applying a flexural/bending load.

The test was performed for Carbon fibre rod, titanium rod, and a joint that included titanium rod inserted into carbon fibre rods as per ASTM D790 standards.

Below are the graphs for all the three specimens taken.

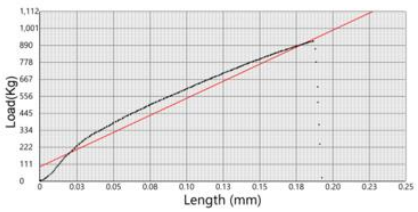

Figure 37: Load vs Deformation graph generated by 3-point bend test for Titanium

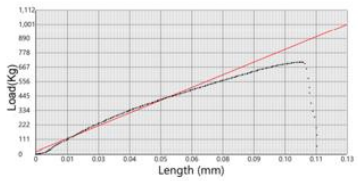

Figure 38: Load vs Deformation graph generated by 3-point bend test for Carbon Fibre

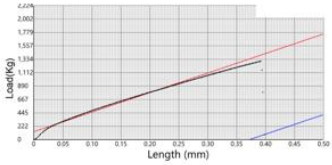

Figure 39: Load vs Deformation graph generated by 3-point bend test for Joint (carbon fibre+ titanium)

Result: The combination of titanium and carbon fibre has the highest strength of around 1300N, hence the same was used at the joints to provide extra strength.

3.2 RPS Testing

The analysis of the Roll-over Protection System was aimed at the verification of design and ensuring rider safety in accordance with the ASME HPVC guidelines. This physical testing was undertaken in our college gym and was performed with the specific loading conditions as mentioned in the guidelines

Figure 40: A top load of 2670N (272Kg) applied to the top of the roll bar, directed downwards.

Figure 41: A side load of 1330N (135Kg) applied to the side of the roll bar at shoulder height.

Result: The RPS meets the required specifications of top and side load deflections

3.2 Wind Tunnel Testing

This was done to verify the simulated results of drag coefficient of ERAWAT, using a scaled 3D printed model of the vehicle.

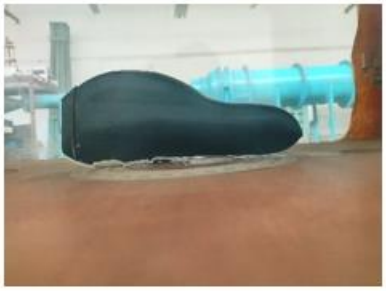

Figure 42: 3D model of fairing inside wind tunnel

Figure 43: Wind Tunnel Machine

Result: The final results of a wind tunnel experiment gave drag coefficient of 0.09 which is close to our simulation results.

4. Conclusion

4.1 COMPARISON – DESIGN GOALS

METRIC	TARGET VALUE	ESTIMATED VALUE
Coefficient of Drag	<0.1	0.06
Field of View	180 Degree	180 Degree
Turning Radius	<6m	Around 4.5m
Cost	<Rs. 5,00,000	Rs. 4,99,300
Rider Satisfaction	8/10	9.5/10
Weight	<30Kg	28 Kg
Rider Hight Range	15 cm	16 cm
Braking Distance from 25 Km/Hr	<6m	4m
Low Speed Stability	Stable at 5 Km/Hr for 50m	Stable at 5 Km/Hr for 55m
Range of Vehicle at 500W Driving Power	>35Km	36Km
0-60 Km/Hr	<16 sec	16.1 sec

Table 6: Target Values v/s Achieved Values for ERAWAT

4.2 EVALUATION

PDS criteria set by the team was regularly modified to make essential design decisions and practical approach was followed. Most of the metrics evaluated meet or exceed the target values. The vehicle easily meets all the constraints set forth by ASME Rule book. Each of the manufacturing stage was accompanied by series of exhaustive testing. ERAWAT meets the team's goal of being a fast, efficient and safer e-HPV.

4.3 RECOMMENDATION

Alternates for windshield should be developed. Timelines should be formed to provide ample time for rider testing and taking into consideration failure of Prototypes. Extensive available text resources should be taken into consideration to make best possible design changes. Funding for the vehicle should be taken care well in advance.

4.4 CONCLUSION

Team Raftaar brings a solution to the problem of sustainable transportation in form of its e-HPV. Now with extra added electric power, the fully faired vehicle is not only fast, but also smoother due to extra added suspension system. The team takes pride in extensive testing done behind to make this a commercially viable alternative to existing vehicle out there.

REFERENCES

1. “Design, Modelling and Analysis of Tilted Human Powered Vehicles”, by Vishal Fegade[1], Gajanan Jadhav[1] and M. Ramachandran, IOP Conference Series: Materials Science and Engineering, Volume 377.
2. Race Car Aerodynamics: Designing for Speed by Joseph Katz.
3. www.recumbents.com
4. “Aerodynamics of Human Powered Vehicle”, by C. R. Kyle and M. D. Weaver *Proceedings of the Institution of Mechanical Engineers, Part A: Journal of Power and Energy*. 2004
5. "Human-Powered Vehicles: An Overview," by H. Duane Mellor and Graeme Philipson, Journal of Human-Environment Systems, vol. 26, no. 2, pp. 79-85, 2003.
6. "Human-Powered Vehicles: A Comprehensive Guide to Riding, Racing, and Building," by Tom McCullough, Ecovelo Publishing, 2012.
7. "Human-Powered Vehicles: Design, Modification, and Performance," by William C. Henderson, Human Kinetics Publishers, 1996.
8. "Human-Powered Vehicles: A Historical and Technological Perspective," by David Gordon Wilson, MIT Press, 1999.
9. "The Science of Cycling: Physiology and Training - Part 2," by Edward Coyle, Sports Medicine, vol. 31, no. 7, pp. 509-527, 2001.
10. "Design and Optimization of Human-Powered Vehicles for Efficient Transportation," by Ian D. Walker, International Journal of Sustainable Transportation, vol. 3, no. 3, pp. 177-194, 2009.
11. "Aerodynamics of Human-Powered Vehicles," by David R. Riley, Progress in Aerospace Sciences, vol. 45, pp. 43-66, 2009.
12. "Human-Powered Vehicles and Sustainable Transportation: A Review and Analysis," by Martin K. Dubois and Timothy J. Kehoe, International Journal of Sustainable Transportation, vol. 4, no. 6, pp. 361-388, 2010.
13. "Design and Performance Analysis of a Human-Powered Vehicle," by Marc D. Pollefeys, et al., Proceedings of the Institution of Mechanical Engineers, Part C: Journal of Mechanical Engineering Science, vol. 228, no. 2, pp. 261-273, 2014.
14. "Human-Powered Vehicles: Energy Efficiency and Sustainability," by Tim Schwanen and Karel Martens, Transportation Research Part D: Transport and Environment, vol. 14, no. 5, pp. 325-335, 2009.
15. K. R. Salter, "Human-Powered Vehicles: A Review of Historical, Technological and Biomechanical Aspects," Journal of Sports Sciences, vol. 19, no. 10, pp. 777-788, 2001.
16. J. N. Rao, "Human-Powered Vehicles: Design, Fabrication, and Performance," Proceedings of the Institution of Mechanical Engineers, Part C: Journal of Mechanical Engineering Science, vol. 219, no. 7, pp. 671-685, 2005.
17. J. C. Villamil and R. S. Sánchez, "Design of Human-Powered Vehicles: A Review," Revista Facultad de Ingeniería, vol. 27, no. 46, pp. 83-96, 2018.
18. G. P. Sutton, "Human-Powered Vehicles," The Journal of Experimental Biology, vol. 207, no. 22, pp. 3879-3884, 2004.
19. A. J. Murdock, "Human-Powered Vehicles," Encyclopedia of Aerospace Engineering, pp. 2281-2295, 2010.

20. R. S. Hurst, "The Design and Optimization of Human-Powered Vehicles," Proceedings of the Institution of Mechanical Engineers, Part C: Journal of Mechanical Engineering Science, vol. 222, no. 12, pp. 2357-2370, 2008.
21. E. P. Popov and A. V. Popov, "Human-Powered Vehicles: Status, Prospects, and Development Trends," Journal of Machinery Manufacture and Reliability, vol. 44, no. 4, pp. 273-283, 2015.
22. S. P. Karnopp, "Human-Powered Vehicles: Past, Present, and Future," Proceedings of the Institution of Mechanical Engineers, Part C: Journal of Mechanical Engineering Science, vol. 217, no. 1, pp. 5-10, 2003.
23. M. A. Sánchez, F. Rodríguez, and A. Rodríguez, "Human-Powered Vehicles: A Review of Their History, Design, and Performance," Renewable and Sustainable Energy Reviews, vol. 13, no. 6-7, pp. 1275-1287, 2009.
24. P. J. Zavada, "Human-Powered Vehicles," in Encyclopedia of Modern Optics, 2nd ed., vol. 2, pp. 411-417, 2018.
25. "Design and implementation of a new drive system for recumbent bicycles" by O. Usta, M. Solmaz, and M. Ercan, published in the Journal of Mechanical Science and Technology in 2016:

Appendices

Appendix A- Performance and testing of braking system in HPVCs .

Introduction :-

Stopping time and stopping distance are critical factors in determining the safety of any vehicle.
For determining the stopping time and stopping distance of a vehicle braking system plays a crucial role .
In this annexure, we are comparing the stopping time and stopping distance of our vehicle with
three different braking systems : - double disc brake , single disc brake , and drum brake .

Methodology:

To determine the stopping time and stopping distance, we conducted a series of braking tests on three different vehicles models, each equipped with one of the three braking systems. We used the same test conditions for each vehicle, including a speed of 20 km/h, a dry asphalt surface, and a driver with consistent braking behavior. We repeated each test five times and took the average values to minimize any outliers.

Testing and observation :-

Stopping time = Reaction time + Braking time
Reaction Time = 0.20-0.30sec
Stopping distance = Reaction distance + Braking distance
Reaction Distance = 1-1.5 meters
Vehicle 1 equipped with double disc brake
Vehicle 2 equipped with single disc brake
Vehicle 3 equipped with drum brake

	Vehicle 1	Vehicle 1	Vehicle 2	Vehicle 2	Vehicle 3	Vehicle 3
TEST	Stopping time	Stopping distance	Stopping time	Stopping distance	Stopping time	Stopping distance
1	1.9	4.4	2.1	4.8	2.4	5.4
2	2.1	4.6	2.2	4.9	2.5	5.7
3	1.8	4.5	2.0	4.5	2.2	5.3
4	1.5	3.9	2.3	5.1	2.8	6

5	2.1	4.7	2.1	4.9	2.3	5.4

Figure 1: Testing of the Vehicles to get a better braking system

Results:-

Double Disc Brake:
Stopping Time : 1.88 sec
Stopping Distance: 4.42 meters
Single Disc Brake:
Stopping Time : 2.14 sec
Stopping Distance: 4.84 meters
Drum Brake:
Stopping Time : 2.44 sec
Stopping Distance: 5.56 meters

Discussion:-

The results clearly show that the double disc brake system provides the shortest stopping time and stopping distance, while the drum brake system has the longest. The single disc brake system is in between the other two. This is because the double disc brake system provides more braking force, which is distributed evenly between the two discs, while the drum brake system provides less braking force, which is distributed unevenly around the circumference of the drum.

Conclusion:-

In conclusion, the choice of braking system can have a significant impact on the stopping time and stopping distance of vehicle. The double disc brake system provides the best performance, while the drum brake system provides the worst.

The single disc brake system is a good compromise between the two. Therefore, in our vehicle we choose the double disc braking system based on their performance requirements and safety standards.

Appendix B – Force, Static, thermal analysis of Braking system

Our objective was to make a type of braking system ,which will store the energy which is dispersed or lost while braking, that is regenerative braking.

This year the braking system is different from the previous one's. The previous teams used V-brakes on the front wheel. This year, disc brakes are used on both the wheels. Unlike v-brakes, the disc brakes provide greater control for braking. Disc brakes are also used as the braking system because they are able to make quick stops during the braking. The disc brakes are located at the axle of the wheel, which will allow the vehicle to stop quickly. In addition, the v- brakes were located very close to the edge of the tire where dirt can accumulate and it was harder for the friction pads to grip the rim. However, the disc brakes are centered at the wheels and if the vehicle rolls over dirt, the disc brakes and friction pads will not be much affected.

For Regenerative Braking, Regenerative supporting Motorcontrollers along with connecting wires are used. During Braking, when brakes are applied microcontrollers disconnect the battery from motor, and make the motor as generator , momentum of the wheels provide energy to the motor thereby storing energy to battery.

Force Analysis

The rotor model heat flux is calculated for the vehicle moving with a velocity 5.5 m/s (20 kmph) and the following is the calculation.

- Mass of vehicle (m) - 30kg
- Initial velocity(u)- 20 km/h = 5.5 m/s
- Final velocity(v)- 0 m/s
- Brake rotor dia.- 160mm
- Axle weight distribution(γ)- 0.35
- Kinetic energy absorbed by disc(f)- 90%
- Acceleration due to gravity(g)- 9.81 m^2 /s
- Coefficient of friction (μ) -0.4

Kinetic energy defined by equation

1. Kinetic energy =(1/2)γ.f.$m(u-v)$ ^{2}/2 = 0.9 × 1/ 2 × 0.35 × 30(27.77 −0)^2/ 2 =71.46J
2. Stopping distance(x)= $u^2/2\mu g$ = 5.5 ^{2}/2*0.4*9.81 = 1.5 m
3. Deceleration time= $v = u + at$
4. t = 1.88 $sec.$

5. Braking power(pb)= $K.E.$ /t=71.46/ 1.88 = 38.01W

Static Thermal Analysis:

Temperature variation was analysed on Ansys 2022, in disk due to heat generation after applying brakes. Maximum temperature was found to be on the outer side of the disc, as brake pads rub on outer side of the disc where friction is high, and it tends to drop as we move to centre .Heat flux is more near the outer end as heat flow from disc to surrounding through convection is more their.

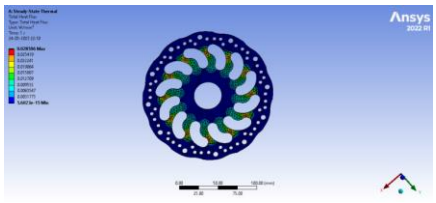

Figure 2: Temperature Variation Distribution

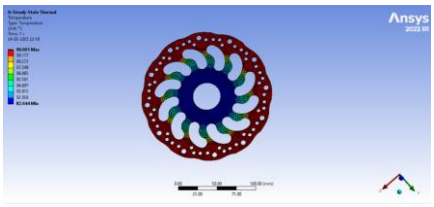

Figure 3: Heat Flux Variation

stress , strain developed in disc was analysed on Ansys 2022. Pressure developed on the outer face (end) is more as it is this place where brake pads rubs with rotor and friction is developed ,which stops the vehicle. Total deformation is again more near the edges, where brake pads are mounted.

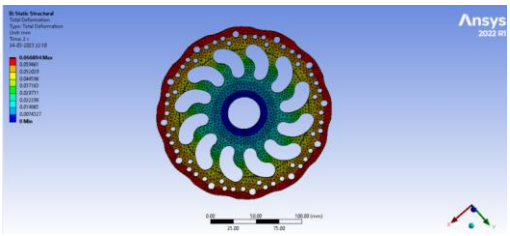

Figure 4: Total deformation variation on disc brake

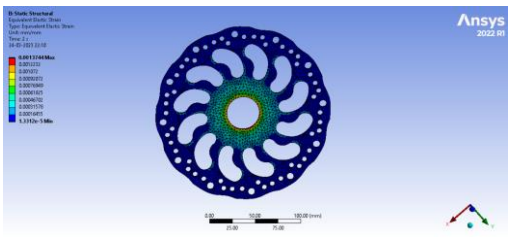

Figure 5: Equivalent Elastic Strain variation

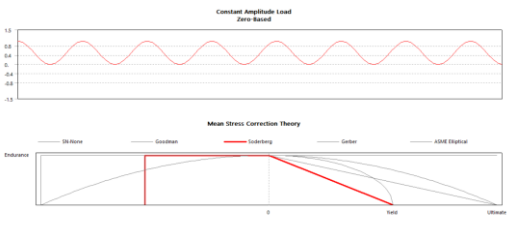

Figure 6: Fatigue Graph

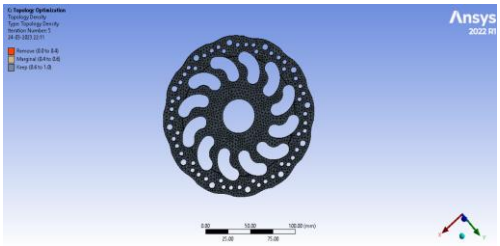

Figure 7: Topology Optimization

Appendix C – Rider Logbook

A maintained record sheet has been provided below: -

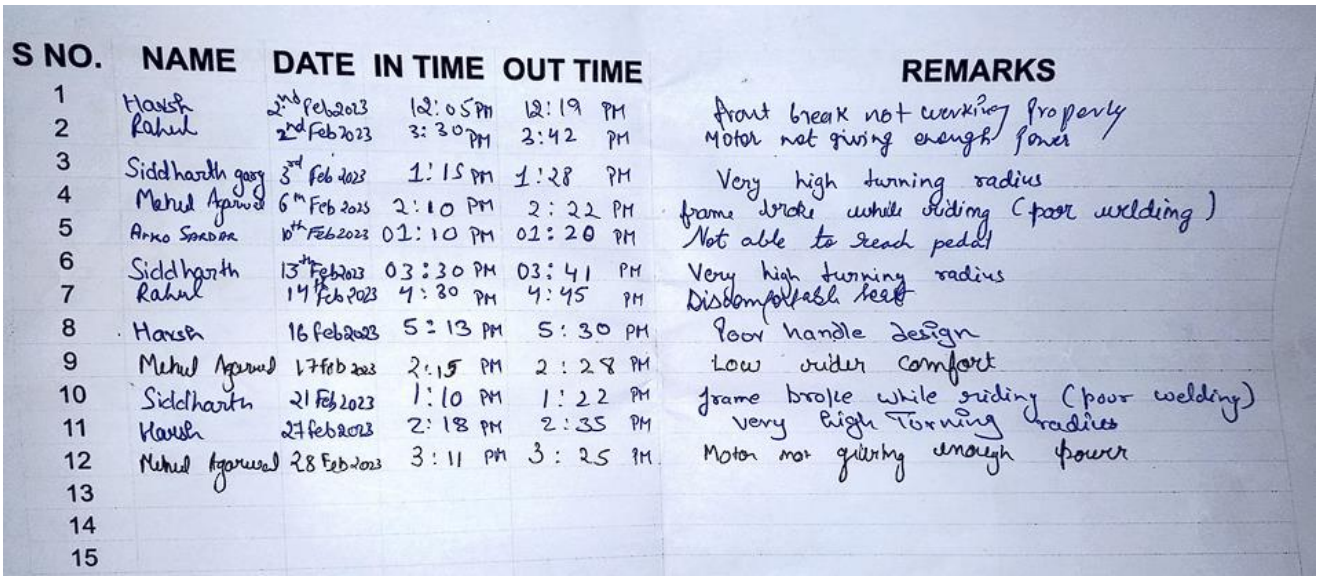

S NO.	NAME	DATE	IN TIME	OUT TIME	REMARKS
1	Harish	2nd Feb 2023	12:05 PM	12:19 PM	Front break not working properly
2	Rahul	2nd Feb 2023	3:30 PM	3:42 PM	Motor not giving enough power
3	Siddharth garg	3rd Feb 2023	1:15 PM	1:28 PM	Very high turning radius
4	Mehul Agarwal	6th Feb 2023	2:10 PM	2:22 PM	frame broke while riding (poor welding)
5	Anko Sarkar	10th Feb 2023	01:10 PM	01:20 PM	Not able to reach pedal
6	Siddharth	13th Feb 2023	03:30 PM	03:41 PM	Very high turning radius
7	Rahul	14th Feb 2023	4:30 PM	4:45 PM	Disbalanced weight
8	Harish	16 feb 2023	5:13 PM	5:30 PM	Poor handle design
9	Mehul Agarwal	17 Feb 2023	2:15 PM	2:28 PM	Low rider comfort
10	Siddharth	21 Feb 2023	1:10 PM	1:22 PM	frame broke while riding (poor welding)
11	Harish	27 feb 2023	2:18 PM	2:35 PM	Very high Turning radius
12	Mehul Agarwal	28 Feb 2023	3:11 PM	3:25 PM	Motor not giving enough power
13					
14					
15					

In this log book, all the problems which were found in the vehicle while testing them has been recorded along with the day of inspection and time when it was inspected.
Once these issues were fixed, they were entered into the different section of the same log book along with the name of the individual who inspected and fixed it.

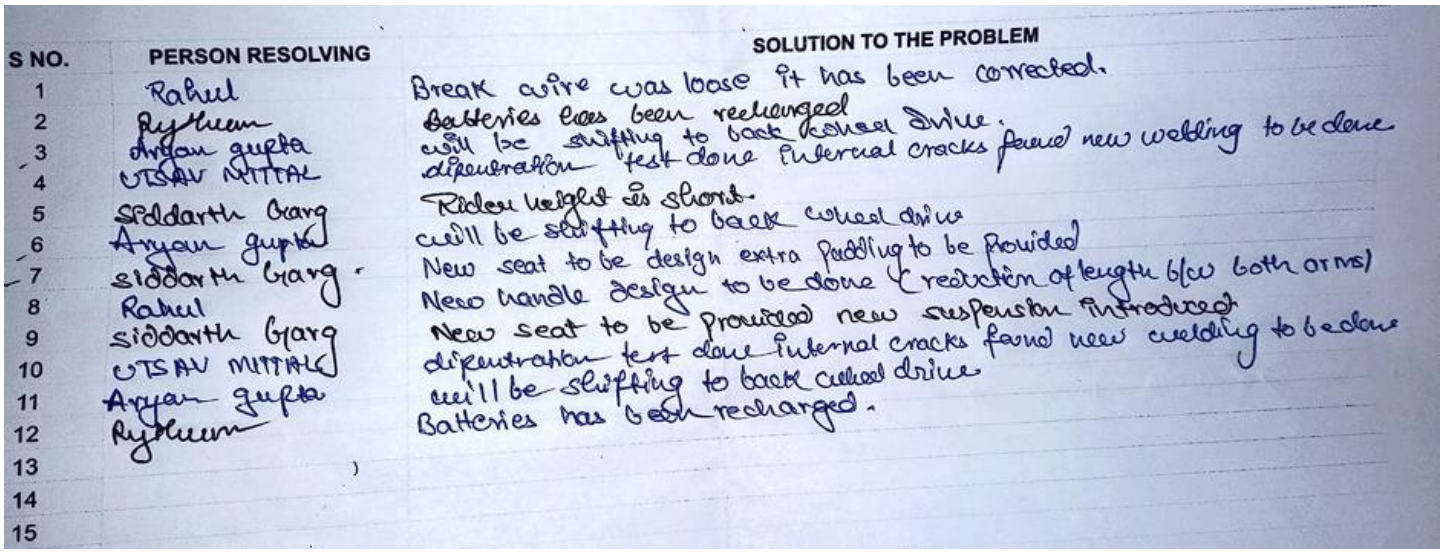

S NO.	PERSON RESOLVING	SOLUTION TO THE PROBLEM
1	Rahul	Break wire was loose it has been corrected.
2	Ryhaan	Batteries has been recharged
3	Aryan gupta	will be shifting to back wheel drive.
4	UTSAV MITTAL	dipenetration test done internal cracks found new welding to be done
5	Siddarth Garg	Rider weight is short.
6	Aryan gupta	will be shifting to back wheel drive
7	siddarth Garg	New seat to be design extra padding to be provided
8	Rahul	New handle design to be done (reduction of length b/w both arms)
9	siddarth Garg	New seat to be provided new suspension introduced
10	UTSAV MITTAL	dipenetration test done internal cracks found new welding to be done
11	Aryan gupta	will be shifting to back wheel drive
12	Ryhaan	Batteries has been recharged.
13		
14		
15		

Appendix D: Placement of Suspension

Research:

Before making the actual vehicle, we analysed the behaviour of our previous model Falcon under loading to determine the points having high stresses. We applied extreme loads on the structure.

- Load applied: 2692.6 N

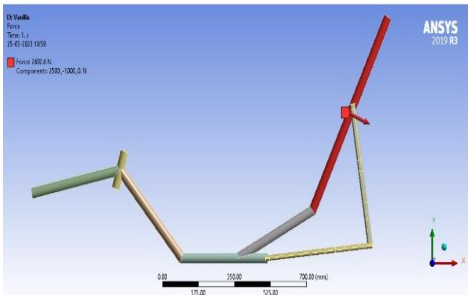

Figure 8: Application of 2692.6 N on previous frame (Falcon)

Conclusion of research:

From this, we discovered that seat stay is having the highest stresses and thus we decided to mount our back suspension on the seat stay. Since we have to place suspension on seat stay, we tried 3 possible positions of suspension on seat stay

- Load applied: 2692.6 N

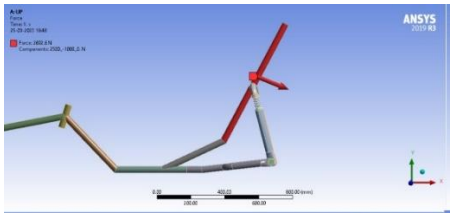

Figure 9: At the top of the seat stay

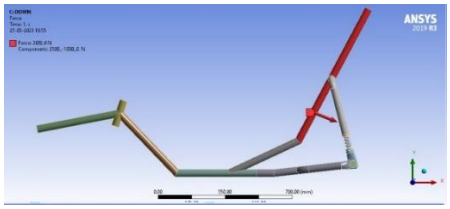

Figure 10: At the bottom of the seat stay

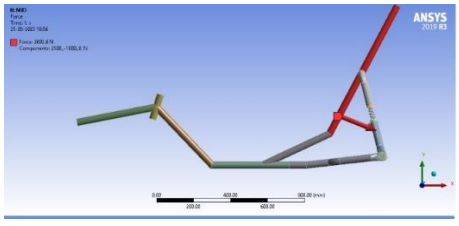

Figure 11: At the middle of the seat stay

Problems Encountered:

The problems discovered in these positions are:

1) There is a bending moment on seat stay on application of load which is lowering the overall strength of the frame.
2) Due to large deflections, there is an interference of main frame with fairing and rear wheel.
3) Two suspensions are required on seat stay which is wastage of resources.

Modification of design:

To encounter these problems, we researched and designed an arrangement which solves the problem without significant loss of performance.

We have installed two thin carbon fibre plates in between the frame and the supporting rods. The seat stay is now not directly connected to the frame but instead connected to the carbon fibre plates through the suspension. By doing so, we made this a three bars structure at the bottom which provides stability. One of the bars containing suspension is having variable length due to which angle at hinge changes resulting in low stress formation.

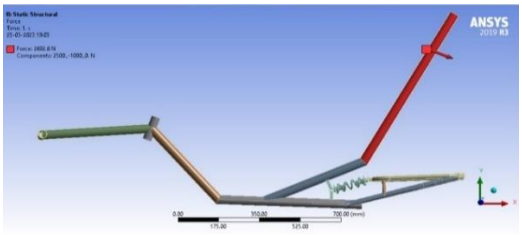

Figure 12: Final placement of suspension

Previous problems are sidelined with the new design as follows:

1. Bending Moment:- We have eliminated the bending moment by providing the hinge joint.

2. We are using a fork-like structure to get benefit of using only 1 suspension

3. Placing the chain stay close to the support rods ensures no interference of rods with wheel or frame.

Figure 13: Final Design

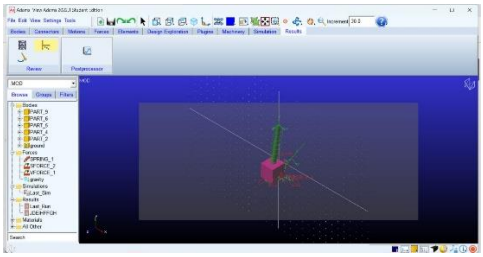

Figure 14: MSC

In MSC Adams, we have performed the load analysis on suspension.

We have calculated spring deformation in which one end of spring is fixed while other is free to move.

Constraint: Deformation must be less than 5 cm.

Preload = 2692.6 N

Spring Constant = 1400lbs/in

Tools used:

- System elements
- Bodies Connector
- Post Processor

Result:

Deformation comes out to be 1.09cm which is well within the constraint.

Front Suspension Analysis:

We have performed load analysis on front suspension in Ansys.

Constraints:

Angle with the vertical = 18 degree,Force is applied at the top.

Parameters: Load = 2500 N Material = Carbon Fibre

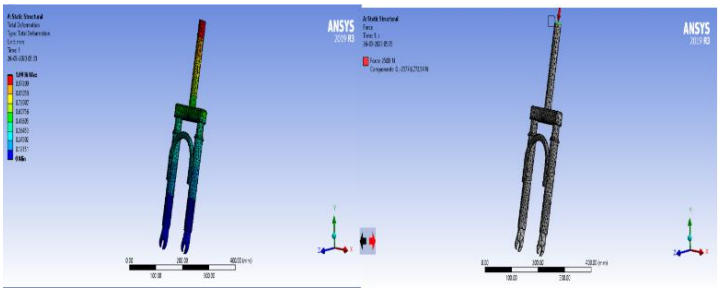

Figure 15: Front Suspension deformation result

Result: A deformation of 1.09mm is noticed.

Calculation of Factor of Safety: We have performed fatigue failure test taking Goodman's theory in consideration to calculate factor of safety.

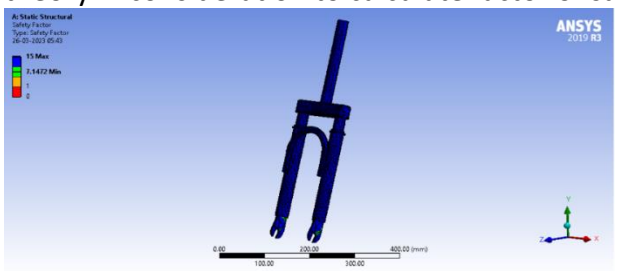

Figure 15: Front Suspension fatigue failure test

Result: Factor of Safety of the whole body is coming out to be 15. The parts which are going to be connected to the wheel hub have Factor of Safety value approximately equal to 7 (can be seen in the figure with green spots)

Appendix E – Crash detection test

Objective

To determine the characteristic curve of a head-on collision of body for the purpose of studying the effectivity of accident-detection module (both algorithmic as well as hardware) using Explicit Dynamics in ANSYS

Introduction

The accident detection module is designed to be lightweight, low-power, easy to replace and quickly installable. It requires being versatile and giving minimum false positives and negatives. The module becomes useless in the case of:

- low sampling rate of accelerometer
- slow response time
- acceleration goes out of detection range
- insufficient sensitivity

To test these conditions a crash test must be done. But it is not feasible as it is expensive, labor-intensive, dangerous to person and lack of appropriate equipments.

Method

A Head-on Collision Crash Test was simulated using Explicit Dynamics on Ansys Software Suite. The results of these simulations gave us an insight into the working of the algorithm of the Accident-Detection Module and also it makes it possible to select appropriate process constants for the module.

It was assumed early in the process that it was not possible to simulate the entire frame and fairing due to the complexity of the problem and the enormous computational resource required to achieve this.

Thus, the following favorable properties for the alternate geometry was proposed:

- It should be a simple geometric shape.
- It should undergo head-on collision to best chance of reproducibility.
- It should have little or no sections that undergo significant deformation as it will give us a chance to see to the fact if the accelerometer can be saturated.
- It should be symmetric.

A hollow cube matches all these criteria. A hollow cube of dimensions 1m x 1m x 1m with a wall thickness of 1mm which is open on the bottom was taken. The velocity of the object was 14m/s and was analyzed for 20ms.

Results

The Deformation was taken as displacement recorded.

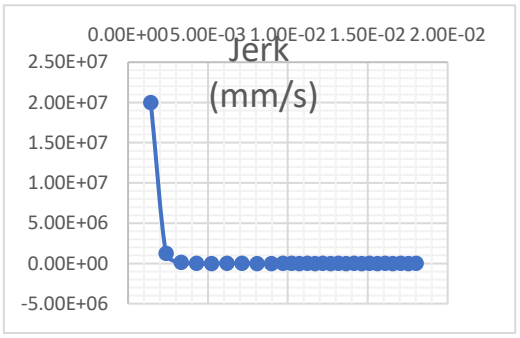

Figure 16: Jerk vs Time graph

Time (s)	Jerk (mm/s³)
1.43E-03	2.00E+07
2.38E-03	1.26E+06
3.33E-03	1.44E+05
4.28E-03	8.09E+03
5.23E-03	-6.87E+03
6.18E-03	4.39E+03
7.13E-03	2.42E+03
8.08E-03	9.85E+02
8.97E-03	-7.05E+03
9.69E-03	7.55E+03
1.02E-02	2.05E+03
1.07E-02	-2.89E+03
1.12E-02	3.64E+03
1.17E-02	-4.08E+03
1.22E-02	4.51E+03
1.27E-02	-4.72E+03
1.32E-02	4.87E+03
1.36E-02	-4.94E+03
1.41E-02	4.99E+03

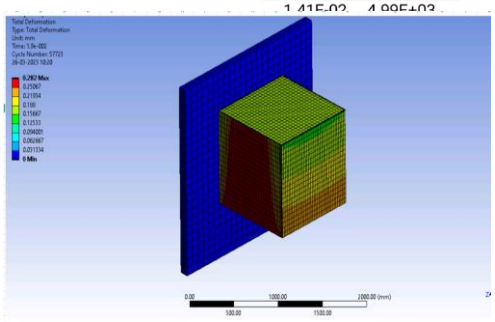

Figure 17: Total deformation under action of head on collision

Conclusion

- We observe that a sampling delay of 2ms is sufficient for successful detection even if it gets saturated in the beginning.
- A critical value for jerk was decided to be 50m/s³
- The Algorithm which depends on cut-off above a critical jerk value would work without issues.

Future direction

It is notoriously difficult to use Arduino-dialect of C++ as a module to further analyze the physical response of the components programmatically by using code modules. Thus we created a python script to make this process easier.

```
import serial, time, math
ser1 = serial.Serial('COMx', 9600)

usleep = lambda x: time.sleep(x/1_000_000.0)

acc_x0 = 0

acc_x1 = 0

acc_y0 = 0

acc_y1 = 0

acc_z0 = 0

acc_z1 = 0

sense = 50

def cast_list(list):

        return list(map("float", list))

while True:

        if ser1.in_waiting:

                packet = ser1.readline()

                line = packet.decode('utf').split("(, )")

                acc_list = cast_list(line)

                acc_x0 = acc_x1

                acc_y0 = acc_y1

                acc_z0 = acc_z1

                usleep(10)

                acc_x1 = acc_list[0]

                acc_y1 = acc_list[1]

                acc_z1 = acc_list[2]

                jerk = math.sqrt(((acc_x1 - acc_x0) ** 2) + ((acc_y1 - acc_y0) ** 2) + ((acc_z1 -
acc_z0) ** 2))

                if jerk > sense :

                        print("%d" %(jerk))
```

Appendix F - Accident alert System SOS and Auto cutoff system code

1. **Accident alert system sos**

```
//team Raftaar asme innovation project 2023

#include<LiquidCrystal_I2C.h>
#include <AltSoftSerial.h>
#include <TinyGPS++.h>

#include <SoftwareSerial.h>
#include <math.h>

#include<Wire.h>
char i2cadd = 0x27
LiquidCrystal_I2C lcd( i2cadd, 16, 2);

//emergency phone number
const String EMERGENCY_PHONE = "ENTER_EMERGENCY_PHONE_NUMBER";

//GSM Module RX pin to Arduino 2
//GSM Module TX pin to Arduino 3
#define rxPin 2
#define txPin 3
SoftwareSerial sim800(rxPin,txPin);

//GPS Module RX pin to Arduino 9
//GPS Module TX pin to Arduino 8
AltSoftSerial neogps;
TinyGPSPlus gps;
```

```
String sms_status,sender_number,received_date,msg;
String latitude, longitude;

#define BUZZER 12
#define BUTTON 11
#define xPin A1
#define yPin A2
#define zPin A3

byte updateflag;

int xaxis = 0, yaxis = 0, zaxis = 0;
int deltx = 0, delty = 0, deltz = 0;
int vibration = 2, devibrate = 75;
int magnitude = 0;
int sensitivity = 20;
double angle;
boolean impact_detected = false;
//Used to run impact routine every 2mS.
unsigned long time1;
unsigned long impact_time;
unsigned long alert_delay = 30000; //30 second

 setup() function : )

void setup()
{

  //Serial.println("Arduino serial initialize");
  Serial.begin(9600);
```

```
//Serial.println("SIM800L serial initialize");
sim800.begin(9600);

//Serial.println("NEO6M serial initialize");
neogps.begin(9600);

pinMode(BUZZER, OUTPUT);
pinMode(BUTTON, INPUT_PULLUP);

//initialize lcd screen
lcd.init();
// turn on the backlight
lcd.backlight();
lcd.clear();

sms_status = "";
sender_number="";
received_date="";
msg="";

sim800.println("AT"); //Check GSM Module
delay(1000);
//SendAT("AT", "OK", 2000); //Check GSM Module
sim800.println("ATE1"); //Echo ON
delay(1000);
//SendAT("ATE1", "OK", 2000); //Echo ON
sim800.println("AT+CPIN?"); //Check SIM ready
delay(1000);
//SendAT("AT+CPIN?", "READY", 2000); //Check SIM ready
sim800.println("AT+CMGF=1"); //SMS text mode
```

```
  delay(1000);
  //SendAT("AT+CMGF=1", "OK", 2000); //SMS text mode
  sim800.println("AT+CNMI=1,1,0,0,0"); /// Decides how newly arrived SMS should be handled
  delay(1000);
  //SendAT("AT+CNMI=1,1,0,0,0", "OK", 2000); //set sms received format
  //AT +CNMI = 2,1,0,0,0 - AT +CNMI = 2,2,0,0,0 (both are same)

  time1 = micros();
  //Serial.print("time1 = "); Serial.println(time1);
  //read calibrated values. otherwise false impact will trigger
  //when you reset your Arduino. (By pressing reset button)
  xaxis = analogRead(xPin);
  yaxis = analogRead(yPin);
  zaxis = analogRead(zPin);

}
 * loop() function
void loop()
{



//every 2mS call impact routine
  if (micros() - time1 > 1999) Impact();

  if(updateflag > 0)
  {
    updateflag=0;
    Serial.println("Impact detected!!");
    Serial.print("Magnitude:"); Serial.println(magnitude);
```

```
  getGps();
  digitalWrite(BUZZER, HIGH);
  impact_detected = true;
  impact_time = millis();

  lcd.clear();
  lcd.setCursor(0,0); //col=0 row=0
  lcd.print("Crash Detected");
  lcd.setCursor(0,1); //col=0 row=1
  lcd.print("Magnitude:"+String(magnitude));
}


if(impact_detected == true)
{
  if(millis() - impact_time >= alert_delay) {
    digitalWrite(BUZZER, LOW);
    makeCall();
    delay(1000);
    sendAlert();
    impact_detected = false;
    impact_time = 0;
  }
}

if(digitalRead(BUTTON) == LOW){
  delay(200);
  digitalWrite(BUZZER, LOW);
  impact_detected = false;
  impact_time = 0;
}
```

```
  while(sim800.available()){
    parseData(sim800.readString());
  }

  while(Serial.available())  {
    sim800.println(Serial.readString());
  }

}

 * Impact() function

void Impact()
{

  time1 = micros(); // resets time value

  int oldx = xaxis; //store previous axis readings
  int oldy = yaxis;  //store previous axis readings
  int oldz = zaxis;  //store previous axis readings

  xaxis = analogRead(xPin);
  yaxis = analogRead(yPin);
  zaxis = analogRead(zPin);



  //loop counter prevents false triggering. Vibration resets if there is an impact. Don't detect new changes until that "time" has passed.
  vibration--;
```

```
 //Serial.print("Vibration = "); Serial.println(vibration);
 if(vibration < 0) vibration = 0;
 //Serial.println("Vibration Reset!");

 if(vibration > 0) return;

 deltx = xaxis - oldx;
 delty = yaxis - oldy;
 deltz = zaxis - oldz;

 //calculate force of impact in Magnitude.
 magnitude = sqrt(sq(deltx) + sq(delty) + sq(deltz));

 if (magnitude >= sensitivity) //impact detected
 {
  updateflag=1;
  // to reset anti-vibration counter
  vibration = devibrate;
 }

 else
 {
  //if (magnitude > 15)
    //Serial.println(magnitude);
  //reset magnitude of impact to 0
  magnitude=0;
 }

}

 parseData() function
```

```
void parseData(String buff){
  Serial.println(buff);

  unsigned int len, index;

  //Remove sent "AT Command" from the response string.
  index = buff.indexOf("\r");
  buff.remove(0, index+2);
  buff.trim();

  if(buff != "OK"){

    index = buff.indexOf(":");
    String cmd = buff.substring(0, index);
    cmd.trim();

    buff.remove(0, index+2);
    //Serial.println(buff);

    if(cmd == "+CMTI"){
      //get newly arrived memory location and store it in temp
      //temp = 4
      index = buff.indexOf(",");
      String temp = buff.substring(index+1, buff.length());
      temp = "AT+CMGR=" + temp + "\r";
      //AT+CMGR=4 i.e. get message stored at memory location 4
      sim800.println(temp);
    }

    else if(cmd == "+CMGR"){
```

```
    //extractSms(buff);
    //Serial.println(buff.indexOf(EMERGENCY_PHONE));
    if(buff.indexOf(EMERGENCY_PHONE) > 1){
      buff.toLowerCase();
      //Serial.println(buff.indexOf("get gps"));
      if(buff.indexOf("get gps") > 1){
        getGps();
        String sms_data;
        sms_data = "GPS Location Data\r";
        sms_data += "http://maps.google.com/maps?q=loc:";
        sms_data += latitude + "," + longitude;

        sendSms(sms_data);
      }
    }
  }

 }
 else{
 //The result of AT Command is "OK"
 }

}
 getGps() Function

void getGps()
{
 // Can take up to 60 seconds
 boolean newData = false;
 for (unsigned long start = millis(); millis() - start < 2000;){
   while (neogps.available()){
```

```
    if (gps.encode(neogps.read())){
      newData = true;
      break;
    }
   }
  }

  if (newData) //If newData == true
  {
   latitude = String(gps.location.lat(), 6);
   longitude = String(gps.location.lng(), 6);
   newData = false;
  }
  else {
   Serial.println("No GPS data is available");
   latitude = "";
   longitude = "";
  }

  Serial.print("Latitude= "); Serial.println(latitude);
  Serial.print("Lngitude= "); Serial.println(longitude);
}
sendAlert() function

void sendAlert()
{
  String sms_data;
  sms_data = "Accident Alert!!\r";
  sms_data += "http://maps.google.com/maps?q=loc:";
  sms_data += latitude + "," + longitude;
```

```
  sendSms(sms_data);
}
```

makeCall() function

```
void makeCall()
{
  Serial.println("calling....");
  sim800.println("ATD"+EMERGENCY_PHONE+";");
  delay(20000); //delay 2 sec
  sim800.println("ATH");
  delay(1000); //delay 1 sec
}
```

sendSms() function

```
 void sendSms(String text)
{
  //return;
  sim800.print("AT+CMGF=1\r");
  delay(1000);
  sim800.print("AT+CMGS=\""+EMERGENCY_PHONE+"\"\r");
  delay(1000);
  sim800.print(text);
  delay(100);
  sim800.write(0x1A); //ascii code for ctrl-26 //sim800.println((char)26); //ascii code for ctrl-
26
  delay(1000);
  Serial.println("SMS Sent Successfully.");
}
```

SendAT() function

```
boolean SendAT(String at_command, String expected_answer, unsigned int timeout){

  uint8_t x=0;
  boolean answer=0;
  String response;
  unsigned long previous;

  //Clean the input buffer
  while( sim800.available() > 0) sim800.read();

  sim800.println(at_command);

  x = 0;
  previous = millis();

  //this loop waits for the answer with time out
  do{
    //if there are data in the UART input buffer, reads it and checks for the asnwer
    if(sim800.available() != 0){
      response += sim800.read();
      x++;
      // check if the desired answer (OK) is in the response of the module
      if(response.indexOf(expected_answer) > 0){
        answer = 1;
        break;
      }
    }
  }while((answer == 0) && ((millis() - previous) < timeout));
```

```
  Serial.println(response);
  return answer;
}
```

2. Auto Cutoff System

```
//team Raftaar asme innovation project 2023
#include <Wire.h>
#include <MPU6050.h>
MPU6050 mpu;
int16_t accelerometer_x, accelerometer_y, accelerometer_z;
int16_t gyroscope_x, gyroscope_y, gyroscope_z;
double angle_x, angle_y, angle_z;
double roll, pitch;

const int relay_pin = 7;
const int tilt_threshold = 30;

void setup() {
  Serial.begin(9600);
  Wire.begin();
  mpu.initialize();
  pinMode(relay_pin, OUTPUT);
}

void loop() {
  mpu.getMotion6(&accelerometer_x, &accelerometer_y, &accelerometer_z,
&gyroscope_x, &gyroscope_y, &gyroscope_z);
  angle_x = atan2(accelerometer_y, accelerometer_z) * 180 / M_PI;
  angle_y = atan2(-accelerometer_x, sqrt(accelerometer_y * accelerometer_y +
accelerometer_z * accelerometer_z)) * 180 / M_PI;
  roll = 0.98 * (roll + gyroscope_x * 0.001) + 0.02 * angle_x;
```

```
  pitch = 0.98 * (pitch + gyroscope_y * 0.001) + 0.02 * angle_y;


  if (pitch > tilt_threshold || pitch < -tilt_threshold || roll > tilt_threshold || roll < -
tilt_threshold) {
    digitalWrite(relay_pin, HIGH);
    Serial.println("Tilt angle exceeded threshold. Engine cut off.");
  }
  else {
    digitalWrite(relay_pin, LOW);
  }
  delay(100);
}
```